Journal of Saudi Chemical Society (2017) **21**, 575–582

King Saud University

Journal of Saudi Chemical Society

www.ksu.edu.sa
www.sciencedirect.com

ORIGINAL ARTICLE

Polyaniline–lead sulfate based cell with supercapattery behavior

Alsadek A. Alguail, Ali H. Al-Eggiely, Branimir N. Grgur *

Faculty of Technology and Metallurgy, University of Belgrade, Karnegijeva 4, 11020 Belgrade, Serbia

Received 18 November 2016; revised 26 December 2016; accepted 8 January 2017
Available online 17 January 2017

KEYWORDS

Hybrid;
Supercapacitors;
Capacitance;
Energy;
Power

Abstract The electrochemically synthesized polyaniline and lead sulfate are investigated as a possible active material of the aqueous based hybrid asymmetric supercapacitors. The electrochemical characteristics of polyaniline (doping-dedoping reactions), as well as electrical characteristics (specific capacitance, capacity, energy, and power) of the $PbSO_4$|PANI cell, are determined. Based on the estimated specific energy and power, it is suggested that investigated cell could be classified as "supercapattery" type of electrochemical power sources.

1. Introduction

It is generally recognized that different types of the supercapacitor devices could be used as a useful storage system, for the electric energy obtained from the renewable and alternative power sources [1]. The classical electrochemical double layer supercapacitors (EDLC), had the advantages that can deliver high power density (in the ranges of kW kg^{-1}) and capability (60–120 s typically), excellent reversibility (90–95%), and very long cycle life ($>10^5$) [2]. Unfortunately, EDLC could store low energy density, typically 3–5 Wh kg^{-1} [3]. In order to improve energy density, different pseudocapacitive electrode materials, based for example on transition metal oxides that can store charge by means of redox-based Faradaic reactions, were usually considered [4]. In principle, pseudocapacitive materials can provide the advanced energy density of ~10 Wh kg^{-1} [5] than EDLCs, particularly in the systems where numerous discreet oxidation states can be formed during charge/discharge, for examples RuO_2 and MnO_2 [6]. But because the pseudocapacitive electrode materials endure physical changes during the charge/discharge they have relatively poor durability in comparison with the different carbonaceous EDLCs electrode materials. Different asymmetric and hybrid supercapacitor systems were investigated in order to improve electric performances [5,7]. A hybrid device based on a battery type electrode and an electrochemical capacitor electrode defined by Cericola and Kötz [8] as an "internal serial hybrid" (ISH) in principle could combine good characteristics of supercapacitors and battery [9]. Recently, such configuration was named "supercapattery" (from: supercapacitors-batteries) [10,11]. Practically, all the electrode materials of the commercial battery systems can be used for the battery-type electrode in the suitable electrolyte, from lead–acid batteries to metal/air

* Corresponding author at: Faculty of Technology and Metallurgy, University of Belgrade, Department of Physical Chemistry and Electrochemistry, Karnegijeva 4, 11020 Belgrade, Serbia. Fax: +381 11 3303681.
E-mail address: BNGrgur@tmf.bg.ac.rs (B.N. Grgur).
Peer review under responsibility of King Saud University.

Production and hosting by Elsevier

http://dx.doi.org/10.1016/j.jscs.2017.01.002

systems, but in practice, metallic compounds like SnO_2, MnO_2 and $LiFePO_4$ are usually investigated [10]. One example of such hybrid system based on electrodeposited PbO_2 on graphite in combination with activated carbon negative electrode in 5.3 mol dm^{-3} H_2SO_4 aqueous solutions was recently investigated by Wang et al. [12]. The authors reported a specific capacitance of 63 F g^{-1} in the voltage window from 1.88 to 0.65 V at 5 C rate. The reported specific energy was in the range of 18–27 Wh kg^{-1} with a specific power in the range of 690–150 W kg^{-1}.

Intrinsically conducting polymers (ICPs) represent a distinct group of pseudocapacitive materials that can accumulate energy via both redox and pseudo-capacitive properties [5,13–17]. The ability of ICPs to store charges originates from a doping-dedoping process, and capability to provide the capacitive response through a fast redox reaction of the conjugated areas of the polymer matrix. The most extensively studied ICPs, due to the low cost of the monomer, easy synthesis and environmental friendliness are polyaniline (PANI) and polypyrrole (PPy) with the wide range of the reported specific capacitance in both aqueous and non-aqueous electrolytes [11,16,17]. Recently, we investigated simple supercapattery like cell based on polypyrrole and lead-sulfate in sulfuric acid based electrolyte [18]. The cell shows battery-like behavior at low discharge currents, e.g. <0.5 A g^{-1}, and supercapacitor-like behavior at a higher discharge currents. Discharge in the specific current range of ~0.1–2.3 A g^{-1} based on the active masses, could provide specific capacity of 90–70 Ah kg^{-1}; specific energy of 60–40 Wh kg^{-1} and specific power in the range of 40–1350 W kg^{-1}, with the specific capacitance of the cell in the range of 300–250 F g^{-1}. This findings inspires us to investigate similar cell, but with polyaniline electrode. The theoretical specific capacitance of PANI is as high as 750 F g^{-1} [17], while the experimentally obtained in the sulfuric acid based electrolytes were reported to be in the range of 200–550 F g^{-1} with potential windows of ~0.8 V [19–21]. The reversible doping-dedoping reaction of the PANI occurred in low pH solutions, pH < 2. Under these conditions, due to corrosion instability limited numbers of electrode materials can be used, for example different carbonaceous materials or lead oxide or sulfate. Hence, the aim of this work was to investigate potential characteristics of the hybrid cell with polyaniline as the positive, typical pseudocapacitive materials and lead-lead sulfate as the negative, typical battery electrode material in sulfuric acid based electrolyte.

2. Materials and methods

Polyaniline (PANI) was synthesized from the aniline monomer (ANI) with concentration of 0.25 M in 1 M H_2SO_4 aqueous solution. Prior to use aniline was distilled under reduced pressure. Synthesis was carried out by the galvanostatic method with the current of 15 mA for 1900s (7.9 mAh) onto a plane graphite electrode with dimensions 1.5 cm × 4 cm, A = 6 cm^2, platinum gauze counter, and saturated calomel as the reference electrode. Lead sulfate was synthesized by the oxidation of the one side of the thin lead foil with dimensions 1.5 cm × 4 cm, A = 6 cm^2, first to spongy lead dioxide, and then by reduction of lead dioxide to lead sulfate. Oxidation was conducted with a current of 9 mA over 450 s (1.125 mAh) in solution contained 1 M H_2SO_4 with the addition of 0.05 M $KClO_4$ as an oxidizing agent [18,22]. Formation of the Pb|$PbSO_4$ electrode was performed in pure 1 M H_2SO_4, by the oxidation of lead sulfate to lead dioxide, and then by reduction of the dioxide to sulfate, and sulfate to pure spongy lead, with a current of 6 mA. Procedure of charge-discharge of lead sulfate to lead and vice versa, was repeated until stable charge-discharge curve was obtained, typically three times. The half-cell reactions, and the determination of the cell performances were conducted in 1 M H_2SO_4.

The electrochemical experiments were conducted using Gamry PC3 potentiostat/galvanostat, in the glass cell with a volume of 100 cm^3, equipped with saturated calomel electrode for potential measurement. The voltage of the cell was recorded using Peak Tech 4390 USB DMM, digital voltmeter connected to PC via USB cable.

For the UV–vis study of as synthesized polyaniline, the product was after synthesis scratched from the graphite electrode surface using a plastic knife, and well ground in an agate mortar. The small amounts of solid product, ~3 mg was added to 10 ml of 1 M H_2SO_4, sonicated in an ultrasound bath for 30 min, and finally, after the precipitation of the larger particles that lasted one hour, 3 ml of the solution was analyzed with an UV–vis LLG uniSPEC 2 spectrometer. For the XRD study of as synthesized $PbSO_4$, the same procedure as for the electrode preparation was applied, only the oxidation was conducted for 2000s, to minimize the influence of pure lead from the electrode bulk. The XRD pattern of the samples was recorded with an Ital Structure APD2000 X-ray diffractometer in a Bragg–Brentano geometry using CuKα radiation and the step-scan mode (range: 15–65° 2θ, step-time: 0.50 s, step-width: 0.02°).

3. Results and discussion

Fig. 1 shows an electrochemical synthesis of polyaniline (PANI) and Pb-$PbSO_4$ active electrode materials on graphite and the thin film lead plane, respectively. Aniline electropolymerization from the aniline monomer (ANI) under galvanostatic conditions occurred at the potentials of ~0.75 V according to the following reaction:

$$n\mathrm{ANI} + n(y/2)\mathrm{SO_4^{2-}} \rightarrow [\mathrm{PANI}^{y+}(\mathrm{SO_4^{2-}})_{y/2}]_n + 2n\mathrm{H^+} + (2+y)ne \quad (1)$$

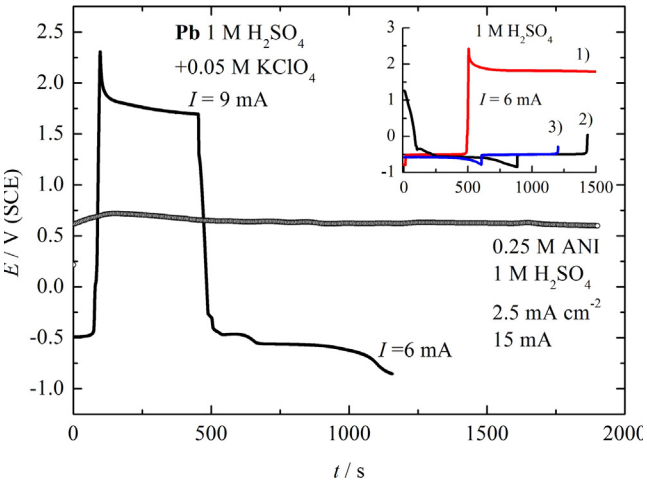

Fig. 1 Galvanostatic formation of the active materials.

where y corresponds to the degree of doping. It was generally accepted that the first step of the polymerization of the aniline, considered as the rate-determining, involves formation of aniline radical cation, followed by coupling and elimination of two protons. After the rearomatization firstly dimer was formed, and further oligomers. The chain propagation occurred by coupling oligomer radical cation with the anilinium radical cation, with simultaneous incorporation of the anions, doping, into the polymer chain [23–25].

Spongy lead sulfate was produced by the galvanostatic oxidation of pure lead to lead dioxide, PbO_2, in 1 M H_2SO_4 with the addition of 0.05 M $KClO_4$ as an oxidizing agent, as shown in Fig. 1 [18,22]. Formed lead dioxide was then reduced to the lead sulfate and lead in the same solution, according to the reactions:

$$PbO_2 + SO_4^{2-} + 4H^+ + 2e \rightleftarrows PbSO_4 + 2H_2O \quad (2)$$

$$PbSO_4 + 2e \rightleftarrows Pb + SO_4^{2-} \quad (3)$$

After washing, the electrode was again oxidized to spongy lead dioxide, but in pure 1 M H_2SO_4, inset in Fig. 1, and then few times reduced to pure lead and oxidized to lead sulfate at the potentials around ~−0.6 V.

The UV–visible absorption spectra of the as synthesized PANI dispersions in 1 M H_2SO_4 aqueous solution, from 190 to 1100 nm are shown in Fig. 2a. Spectra exhibit the local absorption maximum at 334 nm that corresponds to π–π* transition of the benzenoid ring. The band observed in the visible region at 426 nm were associated with the presence of polaron state (charged cation radical, quinoid form) and assigned to polaron−π*, so called exciton [26]. Broad absorption above ~550 nm was associated with polaronic structures in the polyaniline, with theoretical absorption maximum at ~ 850 nm, corresponding to π−polaron transitions. Hence, it can be concluded that as synthesized polyaniline was in the polaronic, emeraldine salt form [27]. In Fig. 2b the XDR spectra of as synthesized lead sulfate are shown. The peaks positioned at 2θ of: 31.21°; 36.16°; 52.11° and 62.09° correspond to the pure lead (JCPDS No. 04-0686 Pb pdf), from the bulk of the electrode. The rest of the observed peaks were in excellent agreement with the peak positions of lead sulfate with anglesite structure (JCPDS No. 36-1461 Anglesite pdf).

In Fig. 3 the cyclic voltammograms of the examined materials are shown. Doping of the PANI in the emeraldine form starts at ~−0.1 V, and proceed up to the potential of ~0.35 V. Above that potential, possible degradation of the PANI could occur [28–30]. The dominant degradation product was proposed to be water soluble benzoquinone with the redox couple of the benzoquinone-hydroquinone [29]. Insoluble and inactive degradation products were suggested to remain on the electrode surface, like PANI strands containing quinoneimine end groups and ortho-coupled oligomers [28,29]. The dedoping reaction of the PANI occurred in the broad potential range, from 0.5 to −0.3 V.

The formal potential of the lead sulfate-lead electrode of −0.55 V was estimated from Fig. 3. Below that potential reduction of the lead sulfate to spongy lead occurred, and above that potential oxidation of lead to lead sulfate, Eq. (3).

In Fig. 4 the charge-discharge curves for investigated materials are shown. A charge of PANI electrode occurred in the potential range of 0.05 V–0.4 V, and discharge from 0.4 to

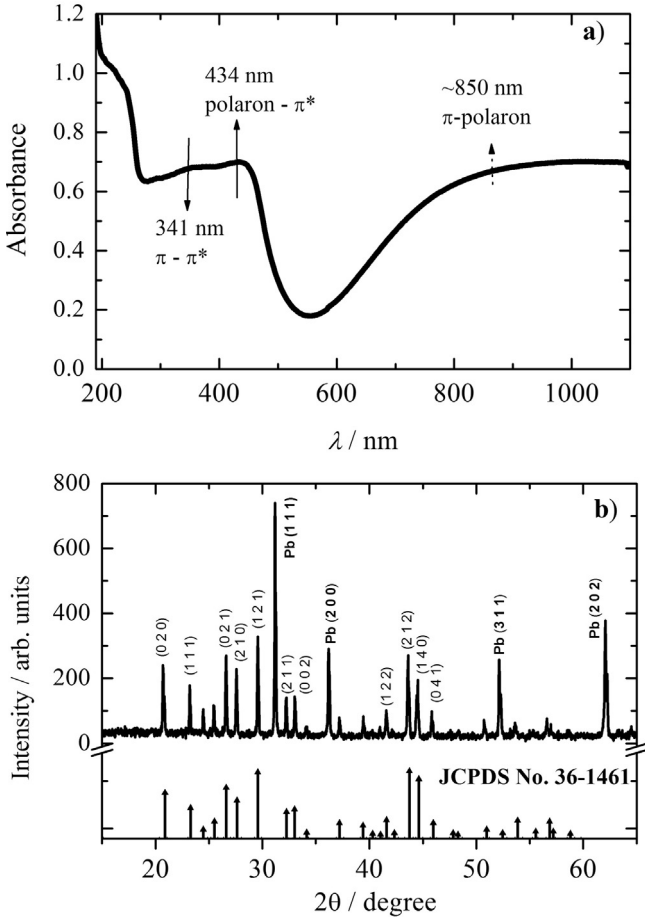

Fig. 2 (a) The UV-visible absorption spectra of the as synthesized PANI dispersions in 1 M H_2SO_4 aqueous solution. (b) The XDR spectra of as synthesized lead sulfate.

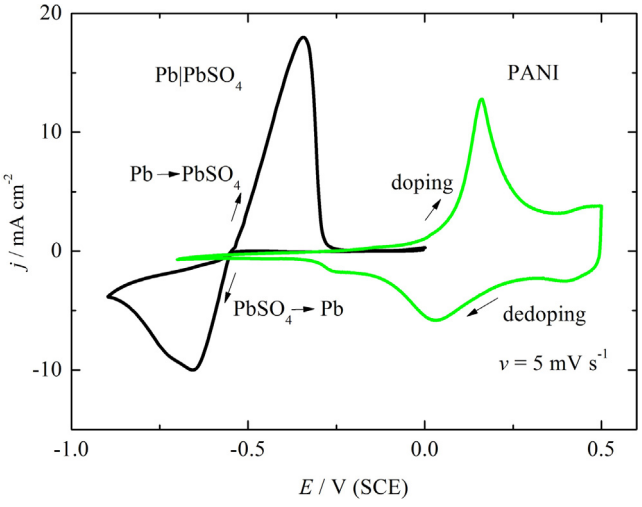

Fig. 3 Cyclic voltammograms of the investigated materials in 1 M H_2SO_4.

−0.15 V, followed by sharp potential decrease caused by diffusion limitations of sulfate anions in dedoping reaction to the −0.4 V. Coulombic efficiency of charge-discharge was around

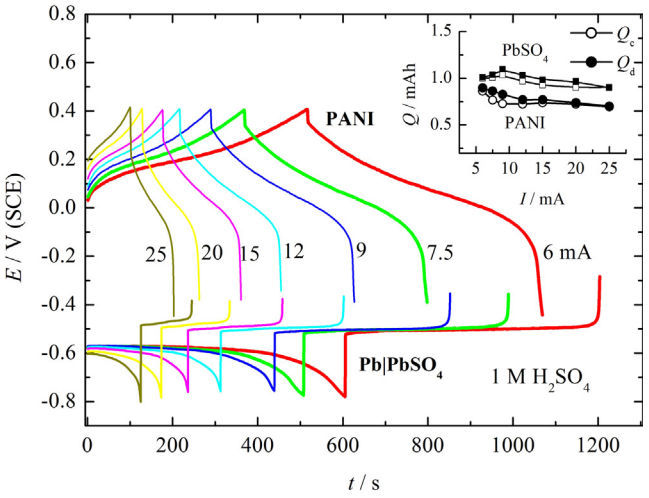

Fig. 4 Charge-discharge curves of the investigated materials for different currents. Inset: obtained charge (open symbols) and discharge (full symbols) capacity for PANI (cycles) and $PbSO_4$ (squares) electrodes.

100%, and obtained discharge electrode capacity depends on applied current ranging from 0.85 mAh for low currents to 0.7 mAh for higher currents, inset in Fig. 4. Reduction of lead sulfate occurred at potentials from ~−0.6 to −0.8 V, while most of the lead oxidation to lead sulfate occurred at potential of ~−0.5 V. The capacity of the charge-discharge was around 1 mAh, inset in Fig. 4.

The polyaniline structure strongly depends on applied potential [31,32]. The potential regions of dominant structures in 0.1 M H_2SO_4 were reported as: −0.2–0.075 V (SCE) leucoemeraldine ($y = 0$); 0.075–0.675 V emeraldine ($y = 0.5$), with substructures: 0.075–0.19 V polaron, 0.19–0.55 V polaron lattice, 0.55–0.675 V bipolaron, and above 0.675 V pernigraniline ($y = 1$) [31]. It was also reported that most of the redox capacitance in 1 M H_2SO_4, ~76%, originated from the PANI polaron structure. Structural analysis of the doping of PANI with divalent anions, to the best of our knowledge, was not treated in the literature. For the single charged anions e.g. chloride, perchlorate etc. the connection of the available (Q) and polymerization charge (Q_p) can be given by the following equation:

$$Q = \frac{y}{2+y} Q_p \tag{4}$$

Hence, for the polymerization charge of 7.9 mAh, corresponding available charge for $y = 0.5$ (polaronic emeraldine state) will be 1.58 mAh, which was almost twice than obtained. Based on the average PANI doping-dedoping charge of ~0.85–0.7 mAh, it could be proposed that divalent sulfate anions were banded to crosslinked parallel polymer chains in the polaron state, as shown in Fig. 5. In that way one polymer unit (consisted of four monomer units) will have a doping degree of 0.5 (emeraldine state), but whole polymer will be doped only with $n \times y/2$ anions.

Based on these considerations, the total polymerization charge, Q_p, of the polyaniline electropolymerization reaction, Eq. (1), is given as:

$$Q_p = I_p t_p = (2+y) neF \tag{5}$$

where y is doping degree. The p-doping/dedoping reaction with sulfate anions is:

$$[\mathrm{PANI}^{y+}(\mathrm{SO_4^{2-}})_{y/2}]_n + (y/2)ne \rightleftarrows [\mathrm{PANI}^0]_n + n(y/2)\mathrm{SO_4^{2-}} \tag{6}$$

and the theoretical available doping/dedoping capacity is given as:

$$Q = It = (y/2)neF \tag{7}$$

Relating Eqs. (5) and (7), available capacity can be connected with polymerization charge with the following equation:

$$Q = \frac{(y/2)}{2+y} Q_p = \frac{(y/2)}{2+y} I_p t_p \tag{8}$$

Consequently, for the polymerization charge of 7.9 mAh, and for the theoretical doping degree of 0.5 (two sulfate anions per polymer units) [17,33], available dedoping charge can be estimated to 0.8 mAh, which was in excellent agreement with experimentally obtained value. For the further calculations of the specific values, it was necessary to calculate the as synthesized PANI mass. The mass of the electropolymerized PANI was related to the total polymerization charge (Q_p), and can be represented, according to the Faraday law, by the following equation:

$$m(\mathrm{PANI}) = \frac{I_p t_p [M_M - 2M(\mathrm{H^+}) + (y/2)M_A]}{(2+y)F} \tag{9}$$

where F is the Faraday constant, M_M and M_A the molar masses of the aniline monomer unit (93.13 g mol^{-1}) and the sulfate anion (96.09 g mol^{-1}), respectively. The mass of the electropolymerized PANI for $y = 0.5$ was estimated to 13 mg. From Eqs. (8) and (9), it was possible to recalculate specific capacity (q) of the doped PANI in the range of 58 mAh g^{-1}. Accordingly, the PANI specific capacitance of 262 F g^{-1}, can be obtained from the following equation:

$$C(\mathrm{PANI}) = \frac{q \times 3600}{\Delta E} \tag{10}$$

where 3600 is to convert Ah g^{-1} in C g^{-1}, and ΔE was discharge potential window, ~0.8 V. On the other hand, the specific capacitance of the $PbSO_4$ electrode in the range of 1600 F g^{-1}, could be estimated for 1 g of $PbSO_4$ and using an equation:

$$C(\mathrm{PbSO_4}) = \frac{nF \times 3600}{M(\mathrm{PbSO_4})\Delta E} \tag{11}$$

where F is Faraday constant (26.8 Ah mol^{-1}), and ΔE was around 0.4 V. Consequently, for serial connection of PANI and $PbSO_4$ electrode, the overall cell capacitance, given as:

$$\frac{1}{C} = \frac{1}{C(\mathrm{PANI})} + \frac{1}{C(\mathrm{PbSO_4})} \tag{12}$$

was in the range of 224 F g^{-1}, suggesting that $C(PbSO_4)$ slightly contributed to the capacitance of the cell. In the same manner the theoretical specific capacity of the cell:

$$\frac{1}{q_{\mathrm{cell}}} = \frac{1}{q(\mathrm{PANI})} + \frac{1}{q(\mathrm{PbSO_4})} = \frac{1}{q(\mathrm{PANI})} + \frac{M(\mathrm{PbSO_4})}{2F} \tag{13}$$

could be estimated to 44 mAh g^{-1}.

Fig. 6 shows charge–discharge curves of the $PbSO_4$|PANI cell for different currents, while limiting the potential of the PANI electrode to 0.4 V. Charge of the cell occurred above

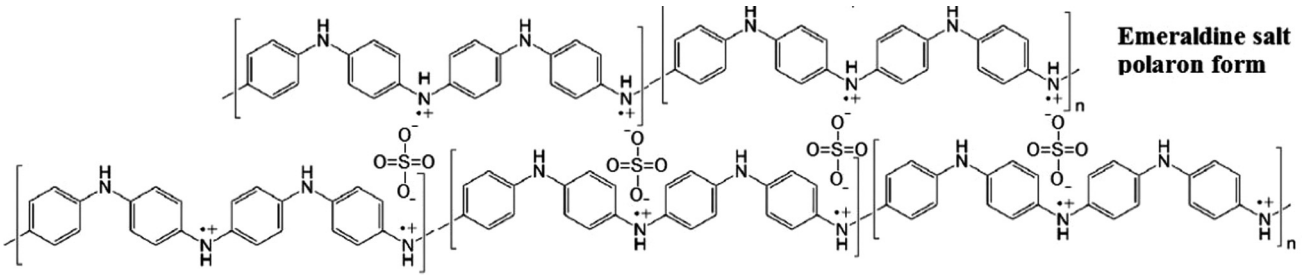

Fig. 5 The proposed structure of polymer chain crosslinking with the sulfate anions in the emeraldine–polaron state of the polyaniline.

0.5 V up to ~0.95 V, while beginning of the discharge voltage, U_d, nonlinearly decreases from 0.85 to 0.65 V with increased applied current, caused by Ohmic drop and polarization resistances of the electrodes, see Fig. 4. Coulombic efficiency (C.E.) slightly decreases from 108% to 101%, inset in Fig. 6, by increased current, probably due reduction of an overoxidized polyaniline products.

In order to determine the nature of relatively high initial voltage drops, the following analysis was performed. In Fig. 7a the electrochemical impedance spectra of the charged cell, using the counter spongy lead electrode as a reference, are shown. Impedance spectra were characterized with small semicircles at higher frequencies, and straight line with the slope near 90° characteristics for pseudocapacitive materials. From the high frequency intercept with Z' axis, the cell resistance of 7.8 Ω was determined. The conductivity of 1 M H_2SO_4 was $26 \times 10^{-2}\,\Omega^{-1}\,cm^{-1}$, so the pure electrolyte resistance (for inter electrode distance of 2 cm and electrode area of 6 cm^2) will be in the range of ~1.3 Ω. Hence, the rest of the resistivity of ~6.5 Ω could be connected with PANI electrode, because resistance of the charged spongy lead can be neglected. Using the determined value of the cell resistance of 7.8 Ω, in Fig. 7 with dotted line is shown theoretical dependence of the voltage drop, IR_Ω, caused only with the Ohmic resistance. Experimentally determined total voltage drop, IR, during discharge, also shown in Fig. 7, point to Ohmic like behavior, with the slope of 13.3 Ω. The total cell resistance, R_{cell}, calculated using the Ohm law slightly depends on applied current, Fig. 7b. Hence, the total cell voltage drop can be given as $I(R_p + R_\Omega)$, where R_p was polarization resistance. The value of R_p, to some extent depends on applied current, Fig. 7b, and can be mainly connected with the increased resistance of the outer surface PANI layer due fast dedoping (discharge) and slow diffusion of the dopant anion from the bulk of the polymer. Also, in some extent the voltage drop during discharge could be also connected with the initial transitions due diffusion controlled solid state reaction of the spongy lead transformation to the lead sulfate.

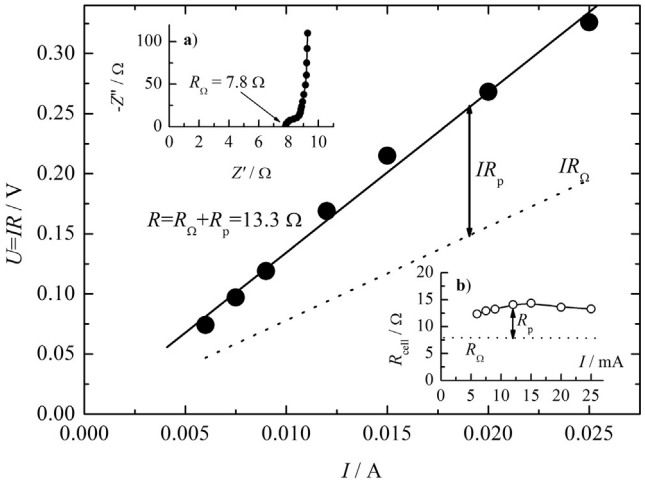

Fig. 7 Experimentally determined voltage drop, IR, during initial cell discharge. Insets: (a) Impedance spectra of charged cell. (b) Calculated total cell resistance using the Ohms law.

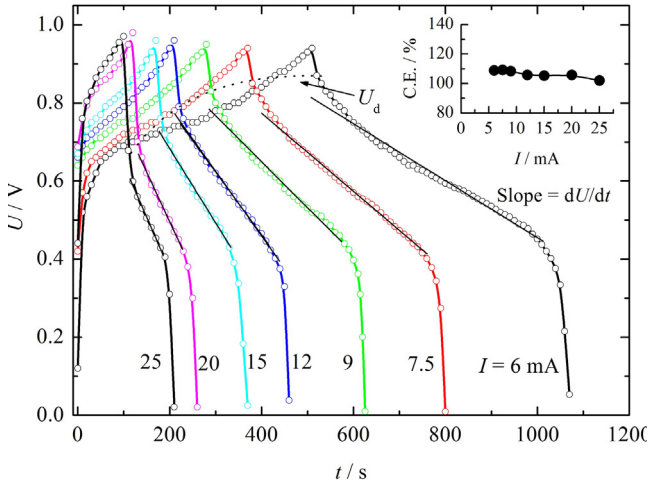

Fig. 6 Charge-discharge curves of the $PbSO_4$|PANI cell for different currents. Inset: Coulombic efficiency of charge–discharge process.

Usually, in the literature the simplified method was used to obtain values of specific capacitances, energy and power. From the determined slopes, dU/dt, during discharge in Fig. 6 the specific capacitance of the cell was estimated by applying the following equation:

$$C_{cell} = \frac{I}{(dU/dt)[m(\text{PANI}) + m(PbSO_4)]} \tag{14}$$

where I, A, was discharge current, m(PANI) estimated PANI mass in a doped state of 13 mg, and $m(PbSO_4)$ was valued by the each discharge current and corresponding times using the Faraday law. The calculated values of the specific capacitances of the $PbSO_4$|PANI cell, ranging around 450 F g^{-1}, shown in Fig. 6a), were practically independent of applied specific current. The obtained values using Eq. (14), seem to be overestimated in the comparison with the theoretically cal-

culated one of 224 F g^{-1}. It is interesting to note that the specific capacitance of the cell practically did not vary with applied current, as usually obtained [34]. From the determined values of the specific capacitances, the maximum specific energy, w_{cell}, Wh kg^{-1}, and power, P_{cell}, W kg^{-1}, was obtained using equations:

$$w_{cell} = \frac{1}{2 \times 3.6} C U_d^2 \quad \text{and} : P_{cell} = \frac{w \times 3600}{t_d} \tag{15}$$

where U_d – was taken from Fig. 6, and t_d was in seconds. The dependence of specific energy and power is shown in Fig. 8, with curve 2, in the form of Ragone plot. By increasing the current, specific energy decreased from 47 to 27 Wh kg^{-1}, while specific power increased from 300 to ~1000 W kg^{-1}.

More reliable method for the determination of specific energy and power of such a cell, at constant specific discharge current, I_d, A g^{-1}, was to use the integral form of specific energy:

$$w_{cell} = \frac{I_d}{3600} \int_0^t U dt \tag{16}$$

and specific power:

$$P_{cell} = \frac{I_d}{\Delta t_d} \int_0^t U dt \tag{17}$$

The calculated values are given with line 1 in Fig. 8. The specific energy decreased from 30 to 20 Wh kg^{-1}, while the specific power increased from 200 to ~800 W kg^{-1}, by increasing specific current. The specific capacitance of the cell in the range of 215–230 F g^{-1}, were calculated using the following equation

$$C_{cell} = \frac{I_d t_d}{U_d} \tag{18}$$

where t_d was in seconds. These values were in good agreement with theoretically calculated of 224 F g^{-1}. Specific capacity of the cell, Fig. 8b), slightly decrease from 47 mAh g^{-1} to 40 mAh g^{-1} by increasing the specific current, which was in good agreement with the theoretical value of 44 mAh g^{-1}. According to the obtained specific energy and power, such device could be classified as a supercapattery cell [10].

The cycling performances of the cell were investigated over 44 cycles, Fig. 9, applying the current of 15 mA (0.864 A g^{-1}), with duration of 200 s for charge and discharge cycle, respectively. For the each discharge curve the capacitance was determined, using the simplified method given by Eq. (14), from the linear part of the discharge curve, Fig. 9a). Plotting the dependence of the obtained specific capacitance over cycle number, the decrease of −0.16 F g^{-1} per cycle was determined. Hence, it could be estimated that from an initial value of 445 F g^{-1}, 20% of capacitance loss will be achieved after ~550–600 cycles. Estimated cycle numbers were in good agreement reported for pure polyaniline electrode [35–38] as well as for pure lead sulfate electrode [39].

Pure polyaniline electrode experience large volumetric swelling and shrinking during charge/discharge process as a result of ion doping and dedoping [40]. This volumetric interchange often leads to structural failure and thus relatively fast capacitance deterioration. Apparently, most polyaniline and polypyrrole based electrodes retain less than 50% of the initial capacitance after ~1000 cycles. Therefore, cycling instability is a major obstacle for practical applications of pure conductive polymer electrodes. Enormous stability improvement of the polyaniline and polypyrrole electrodes was recently achieved by Liu et al. [41] depositing a thin carbonaceous shell onto polymer surface, by a hydrothermal reaction using glucose as carbon precursor. Carbonaceous shell-coated polyaniline and polypyrrole electrodes reached remarkable capacitance retentions of ~95 and ~85% after 10.000 cycles. On the other hand, it was reported that 80% of the capacity loss occurred after approximately 450–500 cycles of pure lead sulfate under deep discharge, ~100 DOD [39]. This could be significantly improved by adding a small amount of the different carbon materials into the active mass of lead sulfate electrode [42,43]. Addition of the carbon materials could also have beneficial effect on the cell resistivity.

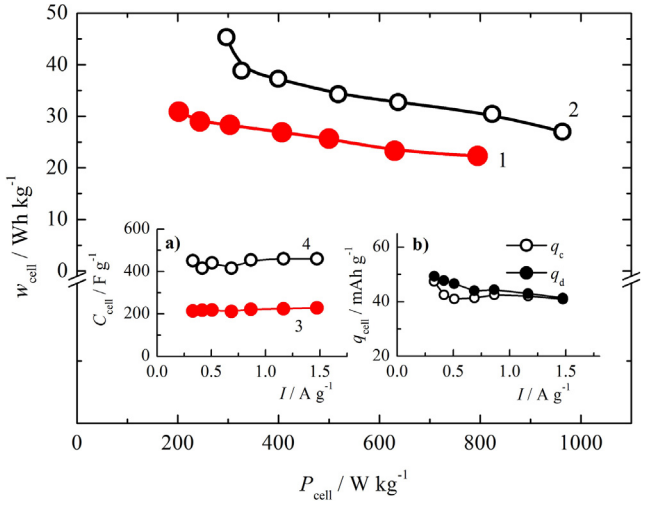

Fig. 8 Ragone plot for $PbSO_4$|PANI cell, values calculate using (1) Eqs. (16) and (17), 2) Eq. (15); (a) The dependence of the specific discharge capacitance calculated using (3) Eq. (18) and 4) Eq. (14); (b) The dependence of the specific capacity on applied specific currents.

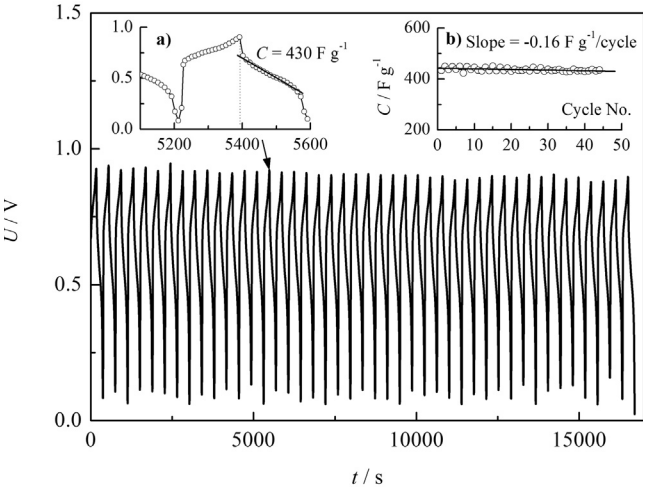

Fig. 9 Cycling behavior of the $PbSO_4$PANI call. (a) The determination of the specific discharge capacitance. (b) The dependence of the specific capacitance on cycle number.

4. Conclusion

The charge–discharge reactions of the electrochemically formed polyaniline ad lead-lead sulfate in 1 M H_2SO_4 were investigated. It was proposed that divalent sulfate anions were banded to crosslinked parallel polyaniline chains in the polaron state. In that way one polymer units (consisted of four monomer units) will have a doping degree of $y = 0.5$ (emeraldine state), but whole polymer will be doped only with $y/2$ anions. The two mathematical methods for the determination of the cell electric characteristic were used: treating the slopes of the charge–discharge curves, and integral form of discharge characteristics. It was shown that integral form of treating was more reliable. The cell capacitance, ranging from 216 F g^{-1} to 230 F g^{-1} was determined, which were in good agreement with theoretically calculated of 224 F g^{-1}. In the specific current range of 0.3–1.5 A g^{-1} based on the active masses, the specific energy decrease from 30 to 20 Wh kg^{-1}, while specific power increased from 200 to ~800 W kg^{-1}. The specific capacity of the cell, slightly decreased from 47 Ah g^{-1} to 40 Ah g^{-1} by increasing the specific current. According to obtained specific energy and power, such device could be classified as a supercapattery cell. From the cyclization experiments, it was estimated that cell will lose 20% of initial capacitance after ~550 cycles. It could be also suggested that improvement of the cycling stability as well as the relatively high resistivity of the cell, can be further achieved preparing a carbonaceous based composite electrode materials.

Acknowledgement

The work was supported by the Ministry of Education and Science of the Republic of Serbia under the research project ON172046. A. A. Alguail and A. H. Al-Eggiely are grateful to the Libyan Ministry of Higher Education and Scientific research, for material supports of their Ph.D. study.

References

[1] L. Guan, L. Yu, G.Z. Chen, Capacitive and non-capacitive faradaic charge storage, Electrochim. Acta 206 (2016) 464–478.
[2] Y. Zhang, H. Feng, X. Wu, L. Wang, A. Zhang, T. Xia, H. Dong, X. Li, L. Zhang, Progress of electrochemical capacitor electrode materials: a review, Int. J. Hydrogen Energy 34 (2009) 4889–4899.
[3] P. Simon, Y. Gogotsi, Materials for electrochemical capacitors, Nature Mat. 7 (2008) 845–854.
[4] X. Zhao, B. Mendoza-Sánchez, P.J. Dobson, P.S. Grant, The role of nanomaterials in redox-based supercapacitors for next generation energy storage devices, Nanoscale 3 (2011) 839–855.
[5] A.K. Shukla, A. Banerjee, M.K. Ravikumar, A. Jalajakshi, Electrochemical capacitors: technical challenges and prognosis for future markets, Electrochim. Acta 84 (2012) 165–173.
[6] Y. Wang, J. Guo, T. Wang, J. Shao, D. Wang, Y.-W. Yang, Mesoporous transition metal oxides for supercapacitors, Nanomaterials 5 (2015) 1667–1689.
[7] P. Xiong, J. Zhu, X. Wang, Recent advances on multi-component hybrid nanostructures for electrochemical capacitors, J. Power Sources 294 (2015) 31–50.
[8] D. Cericola, R. Kötz, Hybridization of rechargeable batteries and electrochemical capacitors: principles and limits, Electrochim. Acta 72 (2012) 1–17.
[9] D.P. Dubal, O. Ayyad, V. Ruiz, P. Gómez-Romero, Hybrid energy storage: the merging of battery and supercapacitor chemistries, Chem. Soc. Rev. 44 (2015) 1777–1790.
[10] L. Yu, G.Z. Chen, Redox electrode materials for supercapatteries, J. Power Source 326 (2016) 604–612.
[11] L. Yua, G.Z. Chen, High energy supercapattery with an ionic liquid solution of $LiClO_4$, Faraday Discuss. 190 (2016) 231–240.
[12] J. Ni, H. Wang, Y. Qu, L. Gao, PbO_2 electrodeposited on graphite for hybrid supercapacitor applications, Phys. Scr. 87 (2016) 045802, http://dx.doi.org/10.1088/0031-8949/87/04/045802.
[13] R. Ramya, R. Sivasubramanian, M.V. Sangaranarayanan, Conducting polymers-based electrochemical supercapacitors-progress and prospects, Electrochim. Acta 101 (2013) 109–129.
[14] G.A. Snook, P. Kao, A.S. Best, Conducting-polymer-based supercapacitor devices and electrodes, J. Power Sources 196 (2011) 1–12.
[15] Y. Shi, L. Peng, Y. Ding, Y. Zhao, G. Yu, Nanostructured conductive polymers for advanced energy storage, Chem. Soc. Rev. 44 (2015) 6684–6696.
[16] E. Frackowiak, V. Khomenko, K. Jurewicz, K. Lota, F. Béguin, Supercapacitors based on conducting polymers/nanotubes composites, J. Power Sources 153 (2006) 413–418.
[17] R. Holze, Y.P. Wu, Intrinsically conducting polymers in electrochemical energy technology: trends and progress, Electrochim. Acta 122 (2014) 93–107.
[18] A.A. Alguail, A.H. Al-Eggiely, M.M. Gvozdenović, B.Z. Jugović, B.N. Grgur, Battery type hybrid supercapacitor based on polypyrrole and lead-lead sulfate, J. Power Sources 313 (2016) 240–246.
[19] J. Ma, Y. Liu, Z. Hu, Z. Xu, Electrochemical synthesis and performance of PANI electrode material for electrochemical capacitor, Ionics 19 (2013) 1405–1413.
[20] H. Qiua, X. Hana, F. Qiua, J. Yanga, Facile route to covalently-jointed graphene/polyaniline composite and it's enhanced electrochemical performances for supercapacitors, Appl. Surf. Sci. 376 (2016) 261–268.
[21] N.H. Khdary, M.E. Abdesalam, G.E. Enany, Mesoporous polyaniline films for high performance supercapacitors, J. Electrochem. Soc. 161 (2014) G63–G68.
[22] B. Petersson, E. Berghult Ahlberg, Thin lead dioxide electrodes for high current density applications in semi-bipolar batteries, J. Power Sources 74 (1998) 68–76.
[23] G. Wallace, G. Spinks, L. Kane-Maguire, P. Teasdale, Conductive Electroactive Polymers, CRC Press, Taylor & Francis Group, Boca Raton, 2009, ISBN 978-1-4200-6709-5.
[24] G. Ćirić-Marjanović, Recent advances in polyaniline research: polymerization mechanisms, structural aspects, properties and applications, Synth. Met. 177 (2013) 1–47.
[25] M.M. Gvozdenović, B.Z. Jugović, J.S. Stevanović, T.Lj. Trišović, B.N. Grgur, Electropolymerization, in: Ewa Schab-Balcerzak (Ed.), Chapter 4: Electrochemical Polymerization of Aniline, InTech publ, 2011, pp. 77–96.
[26] H. Xia, Q. Wang, Synthesis and characterization of conductive polyaniline nanoparticles through ultrasonic assisted inverse microemulsion polymerization, J. Nanopart. Res. 3 (2001) 401–411.
[27] T. Li, Z. Qin, B. Liang, F. Tian, J. Zhao, N. Liu, Morphology-dependent capacitive properties of three nanostructured, polyanilines through interfacial polymerization in various acidic media, Electrochim. Acta 177 (2015) 343–351.
[28] H.N. Dinh, J. Ding, S.J. Xia, V.I. Birss, Multi-technique study of the anodic degradation of polyaniline films, J. Electroanal. Chem. 459 (1998) 45–56.
[29] D.E. Stilwell, S.-M. Park, Electrochemistry of conductive polymers IV: electrochemical studies on polyaniline degradation – product identification and coulometric studies, J. Electrochem. Soc. 135 (1988) 2497–2502.

[30] A.Q. Zhang, C.Q. Cui, J.Y. Lee, Electrochemical degradation of polyaniline in $HClO_4$ and H_2SO_4, Synth. Met. 72 (1995) 217–223.
[31] A.Q. Contractor, V.A. Juvekar, Estimation of equilibrium capacitance of polyaniline films using step voltammetry, J. Electrochem. Soc. 162 (7) (2015) A1175–A1181.
[32] L. Zhuang, Q. Zhou, J. Lu, Simultaneous electrochemical–ESR–conductivity measurements of polyaniline, J. Electroanal. Chem. 493 (2000) 135–140.
[33] M. Magnuson, J.-H. Guo, S.M. Butorin, A. Agui, C. Såthe, J. Nordgren, The electronic structure of polyaniline and doped phases studied by soft X-ray absorption and emission spectroscopies, J. Chem. Phys. 111 (1999) 4756–4764.
[34] Y. Zhao, C.-A. Wang, Nano-network MnO_2/polyaniline composites with enhanced electrochemical properties for supercapacitors, Mater. Design 97 (2016) 512–518.
[35] J. Mu, G. Ma, H. Peng, J. Li, K. Sun, Z. Lei, Facile fabrication of self-assembled polyaniline nanotubes doped with D-tartaric acid for high-performance supercapacitors, J. Power Sources 242 (2013) 797–802.
[36] H. Wang, D. Liu, X. Duan, P. Du, J. Guo, P. Liu, Facile preparation of high-strength polyaniline/polyvinyl chloride composite film as flexible free-standing electrode for supercapacitors, Mater. Design 108 (2016) 801–806.
[37] D. Gui, C. Liu, F. Chen, J. LiuSchool, Preparation of polyaniline/graphene oxide nanocomposite for the application of supercapacitor, Appl. Surf. Sci. 307 (2014) 172–177.
[38] S. Saranyaa, R. Kalai Selvana, N. Priyadharsinia, Synthesis and characterization of polyaniline/$MnWO_4$ nanocomposites as electrodes for pseudocapacitors, Appl. Surf. Sci. 258 (2012) 4881–4887.
[39] Y. Liu, P. Gao, X. Bu, G. Kuang, W. Liu, L. Lei, Nanocrosses of lead sulphate as the negative active material of lead acid batteries, J. Power Sources 263 (2014) 1–6.
[40] G. Wang, L. Zhang, J. Zhang, A review of electrode materials for electrochemical supercapacitors, Chem. Soc. Rev. 41 (2) (2012) 797–828.
[41] T. Liu, L. Finn, M. Yu, H. Wang, T. Zhai, X. Lu, Y. Tong, Y. Li, Polyaniline and polypyrrole pseudocapacitor electrodes with excellent cycling stability, Nano Lett. 14 (2014) 2522–2527.
[42] E. Ebner, D. Burow, A. Börger, M. Wark, P. Atanassova, J. Valenciano, Carbon blacks for the extension of the cycle life in flooded lead acid batteries for micro-hybrid applications, J. Power Sources 239 (2013) 483–489.
[43] D. Pavlov, P. Nikolov, Capacitive carbon and electrochemical lead electrode systems at the negative plates of lead–acid batteries and elementary processes on cycling, J. Power Sources 242 (2013) 380–399.